

High Mass Star Formation: A review

Paolo Persi*

INAF/IAPS, Roma, Italy

E-mail: paolo.persi@inaf.it

This review gives the state-of-art knowledge of high mass star formation gained from observational surveys from millimeter to near-infrared wavelengths. In particular a giant molecular cloud (NGC 6334) is taken as an example of a study of high mass star formation regions including Herschel, Spitzer and near-infrared data.

Frontier Research in Astrophysics - III (FRAPWS2018)

28 May - 2 June 2018

Mondello (Palermo), Italy

*Speaker.

1. Introduction

The formation of massive stars (OB stars with masses greater than $8 M_{\odot}$) in our Galaxy is quite complex and requires good observational knowledge about star-forming environments.

Unlike the case for low-mass stars, there is no observational evolutionary sequence which is firmly established for high-mass star formation. One of the main differences between high-mass and low-mass stars is that the radiation field of a massive star plays a more important role during its whole life and already in its formation phase. Theoretically, a massive proto-stellar embryo heats and eventually ionizes the gas of its surrounding envelope, creating an HII region which develops by expanding within the cloud.

The main review articles of the high mass star formation theories are reported by [1], [2], [3], [4]. Very recently a review of high-mass star and massive cluster formation in the Milky Way based on the recent surveys in the far- infrared (Herschel/Hi-GAL), mid-IR (Spitzer/GLIMPSE) and sub-millimeter (ATLASGAL) has been reported by [5]. In this review is also illustrated a schematic evolutionary diagram proposed for the formation of high-mass star extracted from [6] and discussed here in the next sections.

In this paper, the observations at different wavelengths of one of the most studied galactic high mass star formation region (NGC 6334) are discussed in order to track a possible evolutionary model of high mass star formation.

2. The giant molecular cloud NGC 6334



Figure 1: A wide field image of the NGC 6334 region. The dark cloud near the upper left edge is Barnard 257. The field of view is approximately $90' \times 65'$. This is a composite $H\alpha$ and broad-band R images, courtesy of Martin Pugh.

NGC 6334 is an optical emission nebula, also known as the "Cat's Paw" and is one of the most complex natural star formation laboratories known in our Galaxy. It extends $32' \times 40'$ across the

sky, corresponding to 15×19 square parsec at a distance from the Sun of 1.75 kpc and is located less than 10° away from the Galactic Center ($l = 351^\circ$, $b = 0.7^\circ$). A review of all the observations obtained before 2008 are reported in [7].

The visible nebula, displayed in Fig.1, is ionized by a small number of lightly reddened O-B0 stars which seem, in projection, to be scattered around the whole complex. The densest zones, including the projected centre of the nebulosity, are aligned parallel to the Galactic plane. Along this ridge, several well separated (typically some $2.5'$ or 2 pc) distinct active star forming regions are located as show the composite Spitzer/IRAC image (Fig. 2 left panel) and the CO map (Fig. 2 right panel) .

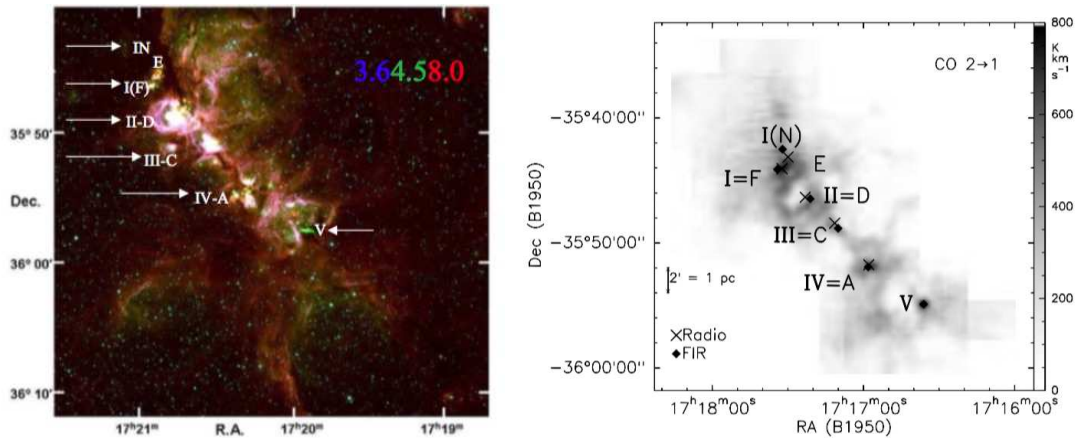


Figure 2: *Left panel:* Spitzer/IRAC color coded image of NGC 6334. The Roman numbers I to V indicate the positions of star formation regions, while the letters show the position of the compact radio sources detected by [8]. *Right panel:* CO(J2-1) map obtained by [9]

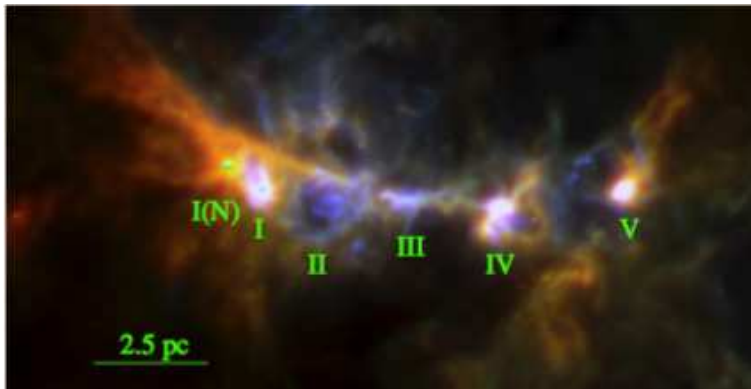


Figure 3: Three-colour Herschel image of NGC 6334 with $500 \mu\text{m}$ data in red, $160 \mu\text{m}$ data in green, and $70 \mu\text{m}$ data in blue taken by [10]. The image is $33'.2 \times 17'.1$. The positions of the five star forming regions are reported.

^{12}CO map obtained by [9] , shows that the molecular gas has a complex filamentary structure along the dense molecular ridge, and that the spots of star formation activity, as signposted by far-infrared maxima, are coincident with molecular line emission peaks.

NGC 6334 was observed by the Herschel space observatory with the PACS and SPIRE instruments

as part of the HOBYS key program. Data were taken in five bands: 70 and 160 μm for PACS at FWHM resolutions or half power beam widths (HPBW) of 5.9" and 11.7", respectively, and 250 , 350 , and 500 μm for SPIRE at FWHM resolutions of 18.2", 24.9", and 36.3", respectively. From the three colour Herschel image of the central part of NGC 6334([10]), result that several young active star-forming regions (labelled I to V) are located in the main filament of the region as reported in Fig.3. Using these HOBYS images, 49 molecular dense cores (MDCs) were extracted by [6] with different characteristics (see Fig.4). Their classification is based on the spectral energy distribution obtained combining the observations at different wavelengths as illustrated in Fig.5. As shown in Fig.4 IR-bright MDCs cluster in the central part of the region whereas IR-quiet protostellar MDCs and starless MDCs candidates are more widely distributed. These different MDCs represent different evolutionary phases of massive star formation.

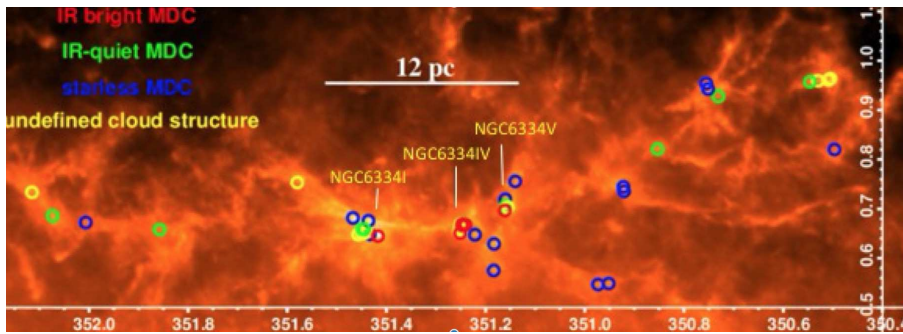


Figure 4: High-resolution (HPBW 18.2'') NH₂ column- density image of the molecular complex taken from [6]. The positions of the MDCs are indicated with a circle.

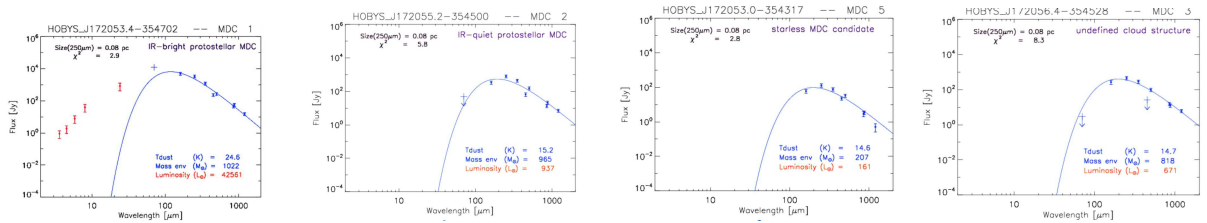


Figure 5: SEDs of IR-bright protostellar MDC, IR-quiet protostellar MDC, starless MDC candidate, and undefined cloud structure.

In the next sub-sections the different regions of star formation are discussed including observations at different wavelengths.

2.1 NGC 6334I

NGC 6334I is the north-east star forming site of the region including two HII regions (E, and F) and the sub-region I(N). Fig.6(Left panel) illustrates the JHK color-coded image of NGC 6334I in which are reported the positions of the different MDCs detected by Herschel. Only one IR-bright MDCs has been found coincident with the HII region F, while in the region I(N) only IR-quiet protostellar MDCs and starless MDCs have been detected. The HII region E with no MDCs appears to

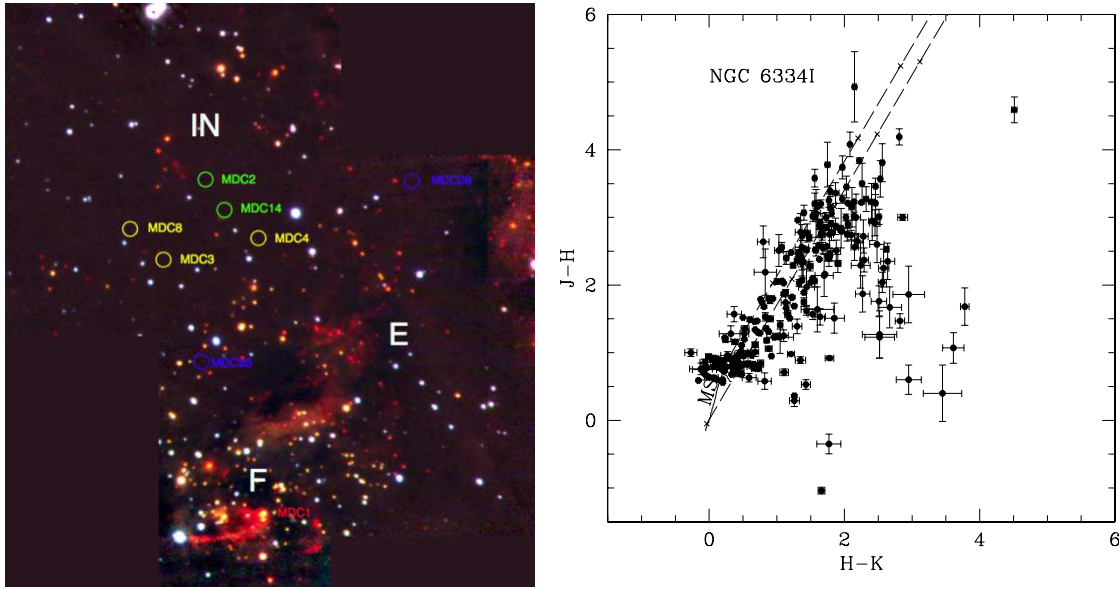


Figure 6: *Left panel:* 196 "×218" RGB-coded image of NGC 6334I made from J (blue), H (green), and Ks (red) mosaics. North is to the top, east to the left (from [7]). *Right panel:* J-H versus H-K digram of the sources detected in the three colours towards NGC 6334 I.

be the most evolved region. The J-H versus H-K diagram reported in Fig. 6(Right panel) indicates the presence of a number of stars with infrared excess suggesting a possible young stellar cluster in the NGC 6334I.

2.1.1 NGC 6334I(F)

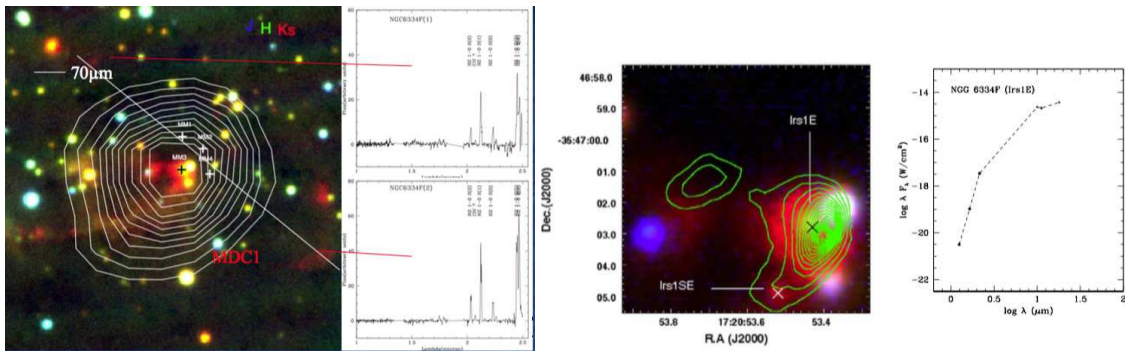


Figure 7: *Left panel:* Color-coded JHKs image of the UCHII region F. The contours represent the Herschel 70 μ m emission of the IR-bright MDC1. The two near-IR spectra are relative to the position of two jets. *Right panel:* The 18 μ m contour map (green lines) from [11] superimposed on the color composite JHKs-band image. The spectral energy distribution of the source IRS1E is shown.

The IR-bright MDC1, found by Herschel coincides with the ultracompact HII region F. At the center of this region, near and mid IR images ([11],[12]) (see Fig.7), show the presence of at least three sources with IR excess. The source IRS1E coinciding with the MDC1 peak, shows a very

steep spectral energy distribution with a spectral index $\alpha_{IR} = 3.8$ and an infrared luminosity $L_{IR} = 3 \times 10^3 L_{\odot}$. (see Fig.7,Right panel) . This high-mass proto-stellar source is considered to be the object most probably responsible for the heating and ionizing of the UCHII region, and for the exciting the H₂ jets present in the region (see Fig.7,Left panel).

2.1.2 NGC 6334I(E)

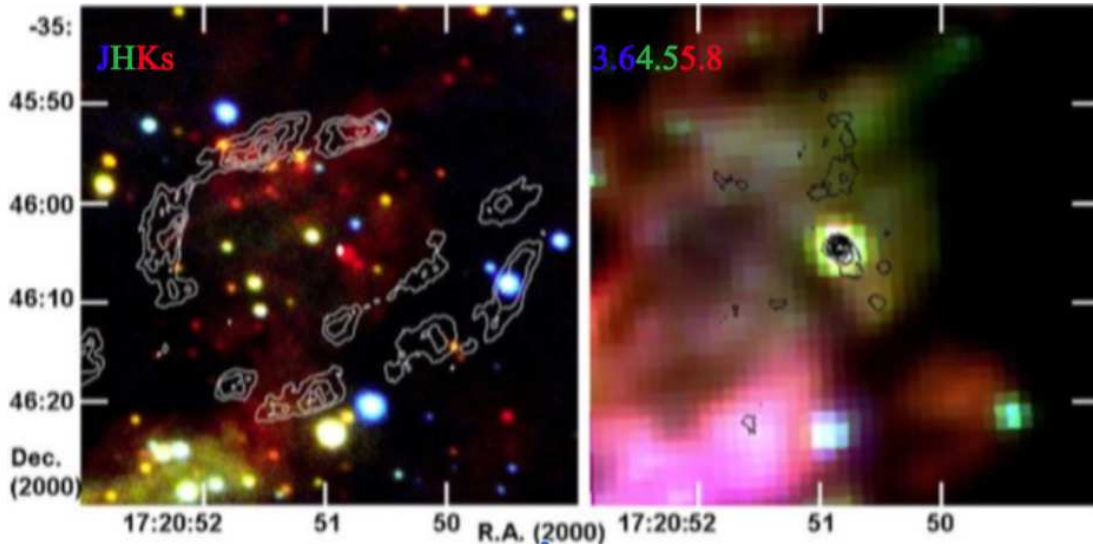


Figure 8: *Left panel:* Composite color coded JHKs image of NGC 6334 E with the 3.5 cm continuum emission contours from [13] overlaid. *Right panel:* Composite color coded Spitzer/IRAC (3.6, 4.5, 5.8 μm) image of NGC 6334 E with the 11.9 μm contours from [14] overlaid.

NGC 6334 E is a spherical and extended (20") HII region detected by [8] that requires an O7.5 ZAMS star to maintain its ionization. The left panel of Fig. 8 shows the 3.5 cm radio continuum contours ([13]) over a color-coded JHKs image. As shows the image at the center of the HII region a number of very red sources with near-IR excess are present ([15]). This indicate that the HII region is probably ionized by a small cluster of at least 12 B0-B0.5 ZAMS stars. Finally at the center of the region is present a source detected at 11.9 μm illustrated in the color-coded Spitzer/IRAC image (see right panel of Fig.8).

The morphology of the HII region NGC 6334 E and the lack of MDCs suggests a state of evolution considerably later than its neighborhoods regions I and I(N).

2.1.3 NGC 6334I(N)

The norther most region of NGC 6334 indicated as I(N) is a dense cold core (2.5' \times 1.5') with a mass of about 2200 M_{\odot} ([17]). Several mm sources were found by [16] (see the contours over the JHKs image of Fig.9). None of the millimeter components have near- or mid-infrared counterparts. Nevertheless, 2.12 μm H₂ emission knot, is observed as show the IR spectrum of Fig.9 (Right panel). Comparison the 1.3mm images taken with ALMA and SMA at different

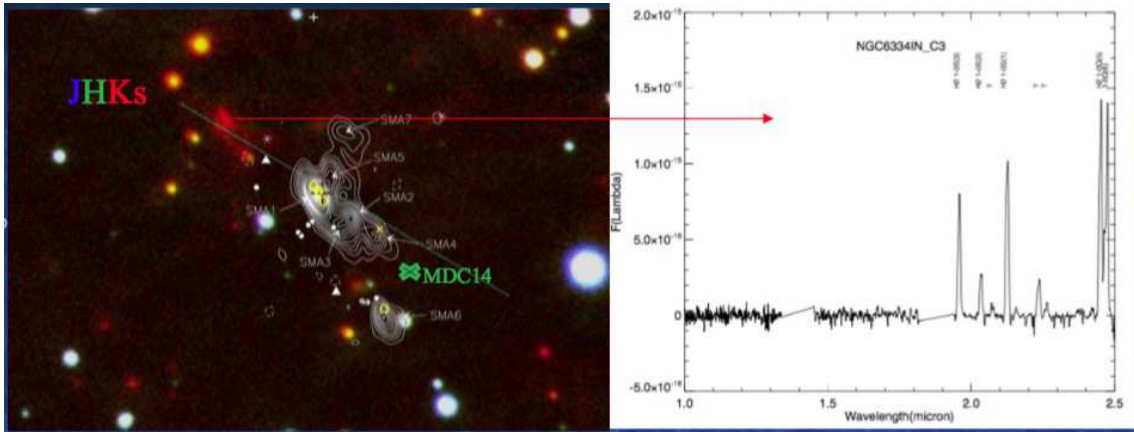


Figure 9: *Left panel:* Color composite JHKs image of a $74'' \times 58''$ field centered on the millimeter source NGC 6334 I(N). The labeled white contours represent the 1.3 mm dust emission from a proto-trapezium-type system discovered by [16] with the SMA. The position of the IR-quiet MDC14 detected by Herschel is shown. *Right panel:* The IR spectrum of the H_2 knot present in this region.

epochs,[18] an outburst in the massive protostellar system MM1 has been discovered. They found that the dust emission from MM1 has increased by a factor of about 4.0 during the intervening years, and undergone a significant change in morphology.

The dominant millimeter source, MM1, is resolved into seven compact ($r=300$ AU) components within a radius of 1000 AU, four of which have brightness temperatures exceeding 200 K, implying minimum luminosities of $10^4 L_{\odot}$ and indicative of central heating [19].

The presence of two IR-quiet molecular dense cores (MDC2, MDC14) in I(N) ([6]), and the near-IR observations reported by [15] indicate that this is the youngest part of NGC 6334 I.

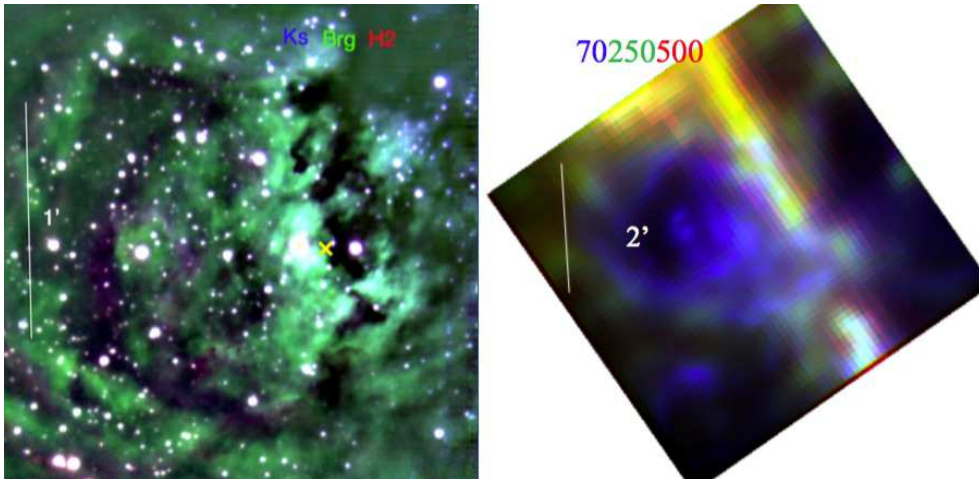


Figure 10: *Left panel:* Composite color-coded KsBr γ H $_2$ image of NGC 6334II-D. North is up, east to the left. *Right panel:* composite color-coded Herschel image of NGC 6334 II-D.

2.2 NGC 6334II-D

NGC6334II-D is dominated by an extended HII region detected by [8]. The radio fluxes

imply at least one ionizing (ZAMS) star of spectral type O6.5 to power the HII region. Extended emission at $3.6 \mu\text{m}$ associated with the HII region was also detected by [20]. The near-IR image is dominated by Br γ emission according to the extension of the HII region (see Fig.10,Left panel). No MDCs have been detected in NGC 6334II-D, and the Herschel image reported in Fig.10(Right panel) show a filamentary structure of the region. These results suggest that NGC 6334 II-D is one of the oldest regions on the molecular ridge, though the expansion of the HII region seems to be triggering a new generation of stars, as in, e.g., S 104 ([21]).

2.3 NGC 6334III-C

This region is characterized by the presence of a non-spherical and extended radio-continuum source mapped by [8] and [22]. An extended Br γ emission is observed in the direction of the HII region (see Fig.11 Left panel) . At the center of the region a young stellar cluster is observed[7]. No known maser emission of any species and no any outflow activity have been observed in NGC 6334III-C. The Herschel images reported in Fig. 11(Right panel) show a filamentary structure with no MDCs detected. Also this region appears in an older evolutionary stage.

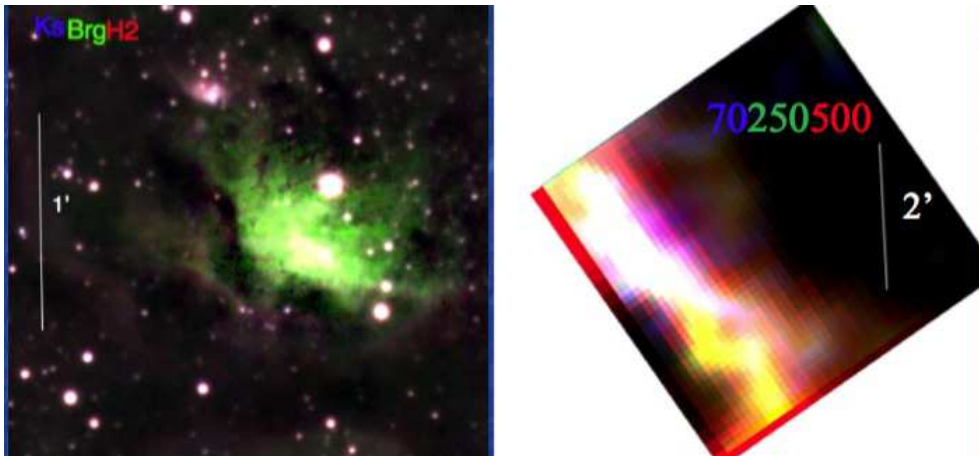


Figure 11: *Left panel:* Composite color-coded KsBr γ H₂ image of NGC 6334III-C. North is up, east to the left.*Right panel:* composite color-coded Herschel image of NGC 6334 III-C.

2.4 NGC 6334IV-A

NGC 6334IV-A is characterized by two large radio bipolar plumes that extend some 2' ([23]) to the north and south (see Fig.12 Right panel). The same bipolar structure is observed from the near to the mid- infrared ([24],[25]). Bright millimeter and sub-millimeter emission has been observed towards the obscured central region (contours in Fig.12 Left panel). In addition two bright young stellar objects (IRS 19 and IRS 20), OH and H₂O masers and several ammonia clumps have been detected. [24] claimed that there is no evidence of a developed stellar cluster, but only of the presence of a small number of luminous (O-B2) young stellar objects. A new centre of active star formation was found to the east of the central region , as indicated by the presence of strong sub- millimeter emission, in particular with the emission peak named MM3 [26] . Three IR-bright

MDCs and one IR-quiet MDC have been detected by Herschel in the central region, while one IR-bright MDC is present in MM3.

This morphology is the result of the effect of massive stellar winds originating from a source at the centre of a dense molecular toroid which, in turn, collimates the outflow material giving rise to two lobes of thermal gas and dust emission.

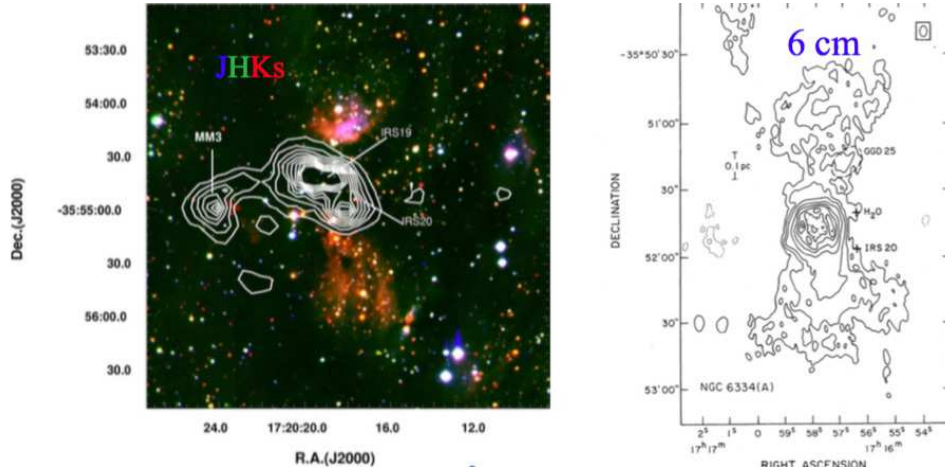


Figure 12: *Left panel:* True color image of NGC 6334 IV made from J (blue), H (green) and Ks (red) individual images from [24]. The contours show the 1.1 mm emission of [26]. *Right Panel:* Radio continuum emission at 6cm detected by [23].

At the position of MM3, [27] detect a near-IR source, (IRS 8E), with a very steep energy distribution with an infrared spectral index of $\alpha_{IR} = 3.5$ and $L_{bol} = 985 L_{\odot}$ (Fig.13, Right panel). This protostar, which coincides with an OH maser source, is the exciting source of two hydrogen molecular knots found in our H₂ image. (Fig.13, Left panel).

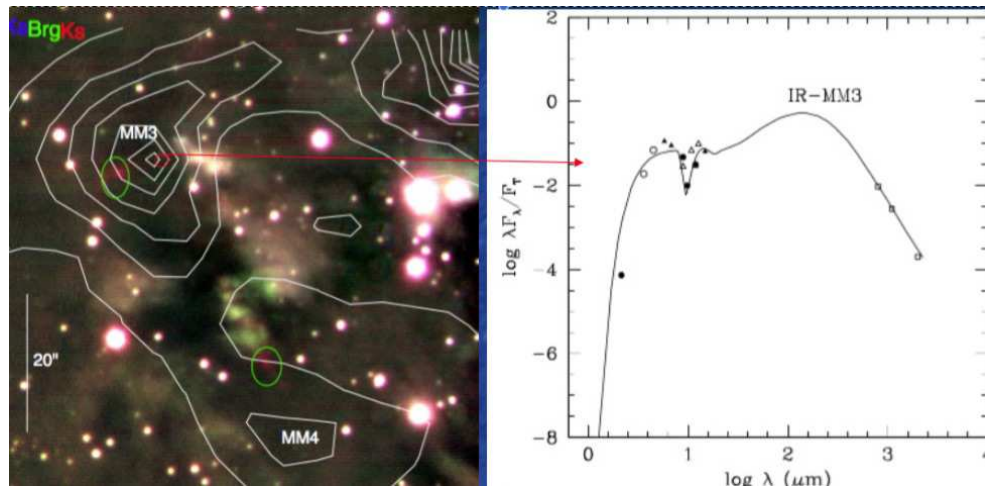


Figure 13: *Left panel:* True color image of MM3 made from Ks (blue), Br γ (green) and H₂ (red) individual images from [27]. The H₂ knots are marked with a green ellipse. *Right Panel:* Spectral energy distribution of MM3.

2.5 NGC 6334V

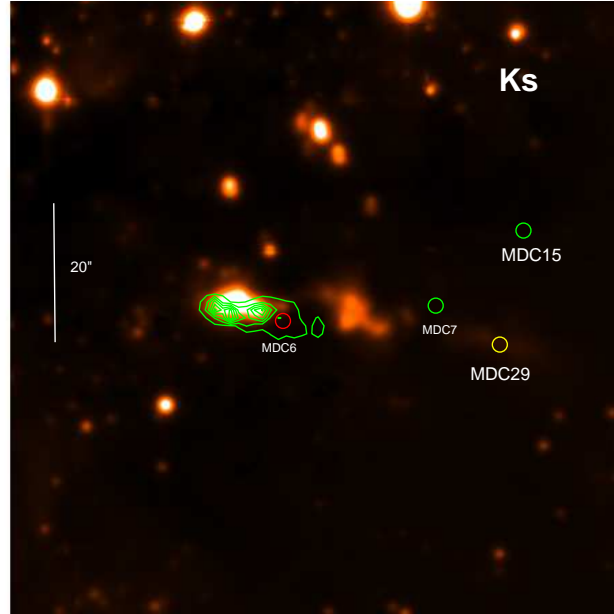


Figure 14: Ks image of NGC 6334V. The contours show the emission at $18.7 \mu\text{m}$, while the circles indicate the positions of the MDCs detected by the Herschel satellite.

NGC 6334 V is the southernmost far-infrared continuum source detected by [28]. Near and mid-IR observations indicate that source V contains several compact dust condensations as well as a near-infrared bipolar nebula within a small region, of size $30'' \times 8''$ (see Fig.14). In addition the region is characterized by the presence of one IR-bright MDC and two IR-quiet MDCs. This suggests that different stages of massive star formation are present in the region.

3. Conclusions

As reported in the previous subsections, in the giant molecular cloud NGC 6334 are present different stages of star formation. The region I(N) without any HII region and with one IR-quiet protostellar MDC is the youngest part of the region, while the region E with the presence of a spherical giant HII region is the oldest part of NGC 6334.

On the base of these kind of observations at different wavelengths, [6] propose a model for the high mass star formation .

This model consist in 6 different phases well described by [5]. Here we report a summary of this model taken from [6]. The different phases are illustrated in Fig.15.

- 1 phase: Massive filaments and spherical clumps, called ridges and hubs, host MDCs (0.1 pc) forming high-mass stars.
- 2 phase: During their starless phase, MDCs only harbor low-mass pre-stellar cores.
- 3 phase: IR-quiet MDCs become protostellar when hosting a stellar embryo of low mass.
- 4 phase: Protostellar envelopes feed from these gravitationally driven inflows, leading to the formation of high-mass protostars.

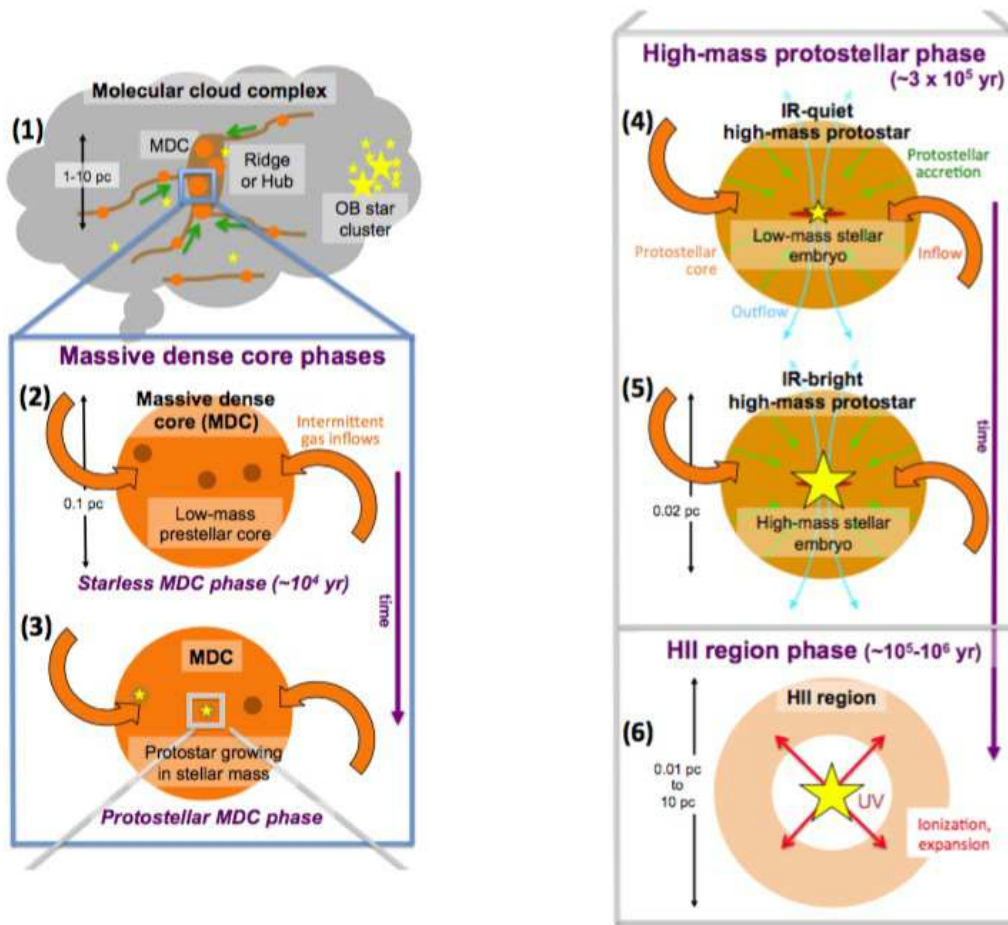


Figure 15: Schematic evolutionary diagram proposed by [6] for the formation of high-mass stars.

5 phase: High-mass protostars become IR-bright for stellar embryos with mass larger than $8M_{\odot}$.

6 phase: The main accretion phase terminates when the stellar UV field ionizes the protostellar envelope and an HII region develops.

According to this model, we could associate the region IN with the phase 3, while the regions IF, II-C and V with the phases 4 and 5. The phase 6 could be represented by the regions IE, II-D and III-C. Finally, in the last years thanks to the Herschel and Spitzer satellites and millimeter and sub millimeter high resolution observations (ALMA) progress have been made on the knowledge of high mass star formation in our Galaxy.

References

- [1] Zinnecker, H., Yorke, H.W., 2007., *ARA&A* 45:481-563
- [2] Beuther, H., Churchwell, E.B., McKee, C.F., Tan, J.C., 2007., *Protostars and Planets V* :165-180
- [3] Tan, J.C., Beltran, M.T., Caselli, P., Fontani, F., Fuente, A., et al., 2014., *Protostars and Planets VI* :149-172

- [4] Krumholz, M.R., 2015., The Formation of Very Massive Stars. In Very Massive Stars in the Local Universe, ed. JS Vink, vol. 412 of Astrophysics and Space Science Library
- [5] Motte, F., Bontemps, S., Louvet, F., 2018., *ARA&A* 56:41-82
- [6] Tigé, J., Motte, F., Russeil, D., et al. 2017, *A&A*, 602 A77
- [7] Persi, P., Tapia, M., 2008 in Handbook of Star forming region Vol II ,Astronomical Society of Pacific p.456
- [8] Rodriguez, L.F., Canto, J., Moran, J.M., 1982, *ApJ*, 255, 103
- [9] Kraemer, K. E., Jackson, J. M. 1999, *ApJS*, 124, 439
- [10] Russeil, D., Schneider, N., Anderson, L. D., et al., 2013, *A&A*, 554, A42
- [11] De Buizer, J.M., Radomski, J.T., Pina, R.K., & Telesco, C. M. 2002, *ApJ*, 580, 305
- [12] Persi, P., Tapia, M., Felli, M., Lagage, P.O., & Ferrari-Toniolo, M. 1998, *A&A* , 336, 1024
- [13] Carral, P., Kurtz, S. E., Rodriguez, L. F., Menten, K., Canto, J., & Arceo, R. 2002, *AJ*, 123, 2574
- [14] Persi P., Tapia M., Roth M., Gomez M., & Marenzi A.R. 2005, in The Dusty and Molecular Universe. A prelude to Herschel and ALMA, ESA SP-577, p.407
- [15] Tapia, M., Persi, P., & Roth, M. 1996, *A&A* , 316, 102
- [16] Hunter, T. R., Brogan, C. L., Megeath, S. T., Menten, K. M., Beuther, H., & Thorwirth, S., 2006, *ApJ*, 649, 888
- [17] Sandell, G. 2000, *A&A*, 358, 242
- [18] Hunter, T. R., Brogan, C. L., MacLeod, G., et al., 2017, *ApJL*, 837, L29
- [19] Brogan, C. L., Hunter, T. R., Cyganowski, C. J., et al., 2016, *ApJ*, 832, 187
- [20] Persi, P. & Ferrari-Toniolo, M. 1982, *A&A*, 112, 292
- [21] Deharveng, L., Lefloch, B., Zavagno, A., et al. 2003, *A&A* , 408, L25
- [22] Brooks, K. J. & Whiteoak, J. B. 2001, *MNRAS* , 320, 465
- [23] Rodriguez, L.F., Canto, J., & Moran, J.M. 1988, *ApJ*, 333, 801
- [24] Persi, P., Tapia, M., & Roth, M. 2000, *A&A*, 357, 1020
- [25] Kraemer, K. E. & Jackson, J. M. 1999, *ApJS*, 124, 439
- [26] Sandell, G. 1999, *A&A*, 343, 281
- [27] Persi, P., Tapia, M., Roth, M. & Gomez, M., 2009, *A&A*, 493, 571
- [28] McBreen, B., Fazio, G. G., Stier, M., & Wright, E. L. 1979, *ApJ*, 232, L183